UNIVERSITY OF WEST BOHEMIA

Applied and Computational Mechanics 1 (2007) 603 - 612

Applied and Computational Mechanics

Nonlinear effects on the rotor driven by a motor with limited power

L. Půst *

Institute of Thermomechanics, Academy of Sciences of CR, Dolejškova 5,182 00 Praha, Czech Republic

Received 10 September 2007; received in revised form 10 October 2007

Abstract

Rotating machines are complicated systems consisting of rotor, stator, driving motor, electric feeding system, etc. Such structures contain many kinds of nonlinearities, both in mechanical and electrical parts. Computing model of the studied system has 4 DOF and the main nonlinearities that are considered are those generated by the driving properties of limited power source and nonlinearities of electric part of motor. Effect of non-ideal source of excitation energy was studied e.g. in [1–5]. Nonlinearities of rotor supports were investigated e.g. in [3, 6]. Here we focus on the influence of nonlinear magnetic flux, with weak smooth nonlinear characteristics. Rotor and its supports are considered as linear. After derivation of differential equations of motion, the effect of different values of nonlinearity of magnetic flux on the mechanical vibration of rotor, on fluctuation of angular velocity and on variation of driving current at constant feeding voltage and at constant loading moment is studied by numerical solutions. Results are presented in the form of time histories and of plane trajectories of main motion variables.

Key words: rotor dynamics, nonlinear oscillations, nonlinear magnetic flux, weak energy source

1. Electro-mechanical nonlinear system

The investigated model of rotor system consists of a disc (mass m [kg]) fixed at mid-span of elastic mass-less shaft and supported on two bearings with the equal stiffness in vertical x and horizontal y directions, fig. 1. The vertical and horizontal stiffness in the centre of shaft including linear stiffness of the bearings supports is k [Nm^{-1}]. The weight of the rotor is mg, which acts vertically in the position of disk. Coefficients of viscous damping b [Nsm^{-1}] are equal in both directions x and y. The elastic rotor is connected with non-ideal driving motor by a torsion stiff clutch and its disk has eccentricity e [m]. The rotor system is loaded by a constant external torsion moment M_z.

Rotor of driving electric motor including disc has moment of inertia I_m [kgm^2]. The stator acts on the rotor by the torsion moment M [Nm] produced by the magnetic flux moment $c\Phi r$ [W$_b$m].The electric components of motor produce the magnetic flux Φ in the electric circuit of motor (inductivity L [H], resistance R [Ω]) in consequence of the current i [A] after connection of voltage U [V] to this circuit. This voltage $U(t)$ regulates the input energy into the whole system; it can be both constant and time variable. The motion of electro-mechanic system, drawn in fig. 1, must be described both in the mechanical part and in the electromagnetic circuit.

* Corresponding author. Tel.: +420 66053212, e-mail: pust@it.cas.cz.

2. Mathematical model of system motion

The forced vibration of the rotor disc D in rectangular coordinates x, y at rotation $\varphi(t)$ is described by two equations

$$\begin{aligned} m\ddot{x} + b\dot{x} + kx &= me(\dot{\varphi}^2 \cos\varphi + \ddot{\varphi} \sin\varphi) + mg \\ m\ddot{y} + b\dot{y} + ky &= me(\dot{\varphi}^2 \sin\varphi - \ddot{\varphi}\cos\varphi) \end{aligned}, \tag{1}$$

where the rotation angle $\varphi(t)$ is supposed to be non-constant with varying velocity $\dot{\varphi}(t)$ and angular acceleration $\ddot{\varphi}(t)$. The linear spring characteristic has compliance $1/k = 1/k_r + 1/2k_s$, where k_r is the stiffness of rotor on rigid supports, k_s is the stiffness of support both in vertical and horizontal directions.

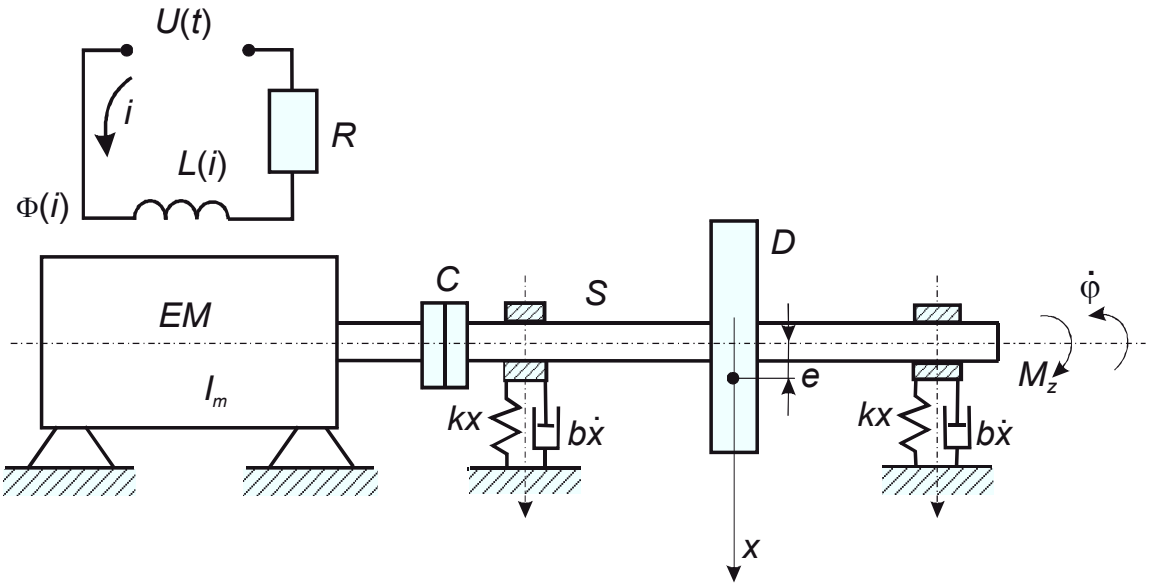

Fig.1. Electro-mechanical rotor system

The energy input to this mechanical subsystem is given by the rotation of rotor with velocity $\dot{\varphi}$ and this rotation is determined by the equation

$$I_m\ddot{\varphi} = -M_z + rc\Phi(i)\,i - b(y\dot{x} - x\dot{y}) - me[\ddot{\varphi}(y\sin\varphi + x\cos\varphi) + \dot{\varphi}^2(y\cos\varphi - x\sin\varphi)] - meg\sin\varphi. \tag{2}$$

Moment of inertia I_m includes the inertia of all rotating parts. On the right side of equation (2), there is M_z external resistance moment constituted e.g. by bearings drag, power take off of working machine, etc. Symbol r is the radius of motor gap, c is structural constant. Product $rc\Phi(i)i$ is active driving electromagnetic moment and presents the moment feeding energy into the mechanical subsystem. It is proportional to current i, which is generated in the electromagnetic circuit controlled by constant or by the time variable voltage $U(t)$ and described for the direct current motor in the simplest form by the following differential equation:

$$L(i)di/dt + Ri + rc\Phi(i)\dot{\varphi} = U(t). \tag{3}$$

The resistance R is here supposed to be constant for the whole range of current i. The inductivity $L(i)$ and magnetic flux $\Phi(i)$change their values with current i. In the first

approximation it suffices usually to apply the linear approximation of these functions:

$$L(i) = L_0 + L_1 i, \quad \Phi(i) = \Phi_0 + \Phi_1 i\,,$$

but this approximation is applicable only for limited range of current i. The examples of better description of magnetic properties are shown in fig. 2a and 2b.

In order to get simpler form of the equations of motion (and more suitable for numerical solution) let us introduce the dimensionless variables. One of the physical magnitudes, which will be constant during the variation of angular velocity and parameters of electric motor is the static shaft deflection x_{st} due to the disk weight mg: $x_{st} = mg/k$. This value and $c\Phi_0 = c\Phi(0)$ are further used as the relative quantities in the dimensionless variables:

$$X = x/x_{st}, \qquad Y = y/x_{st}, \qquad \tau = t\sqrt{k/m}\,, \qquad \beta = b/\sqrt{km}\,, \qquad \varepsilon = e/x_{st}\,,$$
$$\Theta = I_m/mx_{st}^2\,, \qquad \mu_z = M_z/(kx_{st}^2)\,, \qquad I = iR\sqrt{m/k}/c\Phi_0\,, \qquad \rho(I) = \Phi(i)/\Phi_0$$
$$\Lambda(I) = L(i)\sqrt{k/m}/R\,, \qquad u = U\sqrt{m/k}/c\Phi_0\,. \tag{4}$$

The equations of motion in the dimensionless form are

$$\begin{aligned}
&X'' + \beta X' + X = \varepsilon(\varphi'^2\cos\varphi + \varphi''\sin\varphi) + 1\\
&Y'' + \beta Y' + Y = \varepsilon(\varphi'^2\sin\varphi - \varphi''\cos\varphi)\\
&\Theta\varphi'' = -\mu_z + \rho(I)I - \beta(YX' - XY') - \varepsilon(\varphi''(Y\sin\varphi + X\cos\varphi) + \varphi'^2(Y\cos\varphi - X\sin\varphi)) - \varepsilon\sin\varphi\\
&\Lambda(I)I' + I + \varphi' = u(\tau)
\end{aligned} \tag{5}$$

Symbol ( )' = d( )/dτ. Variable φ does not change at dimensionless transformation.

The first and second equations (5) contain more than one second derivative of the variables X, Y and φ in each equation. For solution using Runge-Kutta procedure, the analytical separation of the expression φ'' is necessary. Let us separate φ'' in the third equation (5)

$$\varphi'' = \frac{-\mu_z + \rho(I)I - \beta(YX' - XY') - \varepsilon\varphi'^2(Y\cos\varphi - X\sin\varphi) - \varepsilon\sin\varphi}{\Theta + \varepsilon(Y\sin\varphi + X\cos\varphi)} \tag{6}$$

and then introduce it into the first and second ones. We get:

$$\begin{aligned}
X'' + \beta X' + X = {}& \varepsilon\Big(\varphi'^2\cos\varphi + \\
&\frac{-\mu_z + \rho(I)I - \beta(YX' - XY') - \varepsilon\varphi'^2(Y\cos\varphi - X\sin\varphi) - \varepsilon\sin\varphi}{\Theta + \varepsilon(Y\sin\varphi + X\cos\varphi)}\sin\varphi\Big) + 1\\
Y'' + \beta Y' + Y = {}& \varepsilon\Big(\varphi'^2\sin\varphi - \\
&\frac{-\mu_z + \rho(I)I - \beta(YX' - XY') - \varepsilon\varphi'^2(Y\cos\varphi - X\sin\varphi) - \varepsilon\sin\varphi}{\Theta + \varepsilon(Y\sin\varphi + X\cos\varphi)}\cos\varphi\Big)
\end{aligned} \tag{7}$$

These equations together with last two equations (5) are applied for solutions of further examples.

3. System nonlinearities

There are several kinds of nonlinearities in different subsystems. Rotor part (left sides of equations 1 or of the first two equations (5)) is supposed to be linear in this contribution. Nonlinear supports of rotor were investigated by many authors, e.g. in [5,6]. Nonlinearities of

the right sides of these expressions are connected with the variable rotation angle velocity $d\varphi/d\tau$ due to the limited power and limited inertia of driving motor. The main nonlinearities of the electric circuit of motor originate from the change of magnetic properties with increasing current. The inductivity *L(i)* and the magnetic flux $\Phi(i)$ change their values with current *i* due to the saturation's effect (in dimensionless variables $\Lambda(I)$ and $\rho(I)$). Approximation by polynomial of current *I* is limited on the small current value. Two examples of approximations for greater currents are shown in fig. 2. The step-form of function $\Phi(i)$ is shown in fig.2a and described by tri-linear characteristics:

$$\Phi = 100 * I, \qquad \text{for} \quad |I| \le I_h = \Phi_m / 100$$
$$\Phi = \Phi_m \operatorname{sgn}(I), \qquad \text{for} \quad |I| > I_h = \Phi_m / 100 \tag{8}$$

for several values of $\Phi_{m,}$ or I_h. An example of a set of smooth characteristics Φ,I is plotted in fig. 2b. Analytical description of such kind of characteristic is

$$\Phi(I) = 2\Phi_m * \arctan(I * \pi / 2) / \pi$$
or $$\Phi(I) = 200 * I_h * \arctan(I * \pi / 2) / \pi . \tag{9}$$

The formula (9) is used in the following calculation.

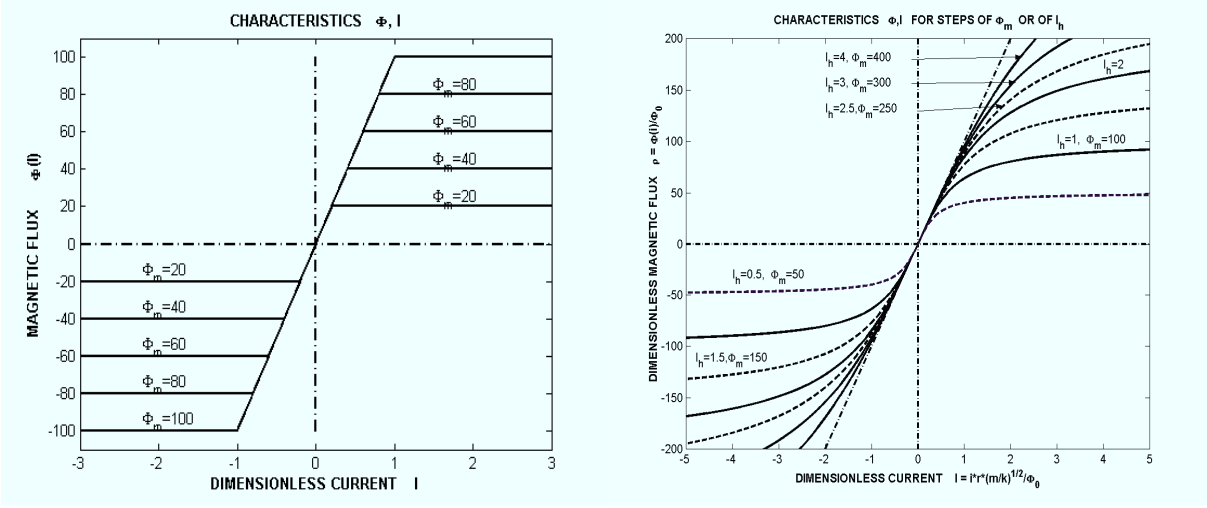

a) b)

Fig. 2. Nonlinear magnetic flux characteristics, a) tri-linear, b) smooth.

4. Examples

For the demonstration of behaviour and properties of investigated rotor system driven by a weak electric motor, we focus on the influence of magnetic nonlinearity given by the smooth characteristics shown in fig. 2b at different values of critical current (saturation) parameter I_h. This parameter determines the current at which the characteristic has approximately the greatest curvature and changes from the increasing function into the rather constant value. Exact speaking, in fig. 2b it is given by the point of intersection of horizontal asymptote and dashed common tangent in the origin of coordinates.

The other parameters and nonlinearities of the whole system will be constant in these examples. Corresponding dimensionless values of these parameters are:

Time interval $\tau = t\sqrt{k/m}$ = 0 – 300, damping $\beta = b/\sqrt{km}$ = 0.05, moment of inertia

$\Theta = I_m / m x_{st}^2$ = 200, eccentricity of unbalance $\varepsilon = e / x_{st}$ = 2, constant torsion load $\mu_z = M_z /(k \mathrm{x}_{\mathrm{st}}^2)$ = 100, reference value of magnetic flux $\rho_0 = r^2 \Phi_0^2 / \left(R x_{st}^2 \sqrt{k\,m} \right)$ = 100, inductivity $\Lambda(I) = L(i)\sqrt{k/m}\,/\,R$ = 4, voltage $u = U\sqrt{m/k}\,/\,r\Phi_0$ = 2.

The results of the first studied case of high current parameter I_h = 4, when the electric circuit is very close to linear one, are plotted in fig.3. The left upper subplot contain the time histories of displacements $X = x/x_{st}$ and $Y = y/x_{st}$ (bottom curve), of velocities $v = \mathrm{d}X/\mathrm{d}\tau$ and $vy = \mathrm{d}Y/\mathrm{d}\tau$ (upper curve). In the middle, there is a component of eccentricity rotation ε*cosφ. Trajectories of displacement and velocities of the centre of rotor disk are plotted in fig. 3b.

From the hurried view in figures 3a and 3b it seems that they present the harmonic oscillations of rotor in axes *X* and *Y*, or stationary rotation with constant angular velocity. But from the fig. 3c showing the course of dimensionless angular velocity η and dimensionless current *I* (again for I_h = 4) it is evident that the current *I* fluctuates in 3% with small ½ harmonic. The angular velocity η fluctuates up to 15 % and contains both ½ and 2 harmonic components.

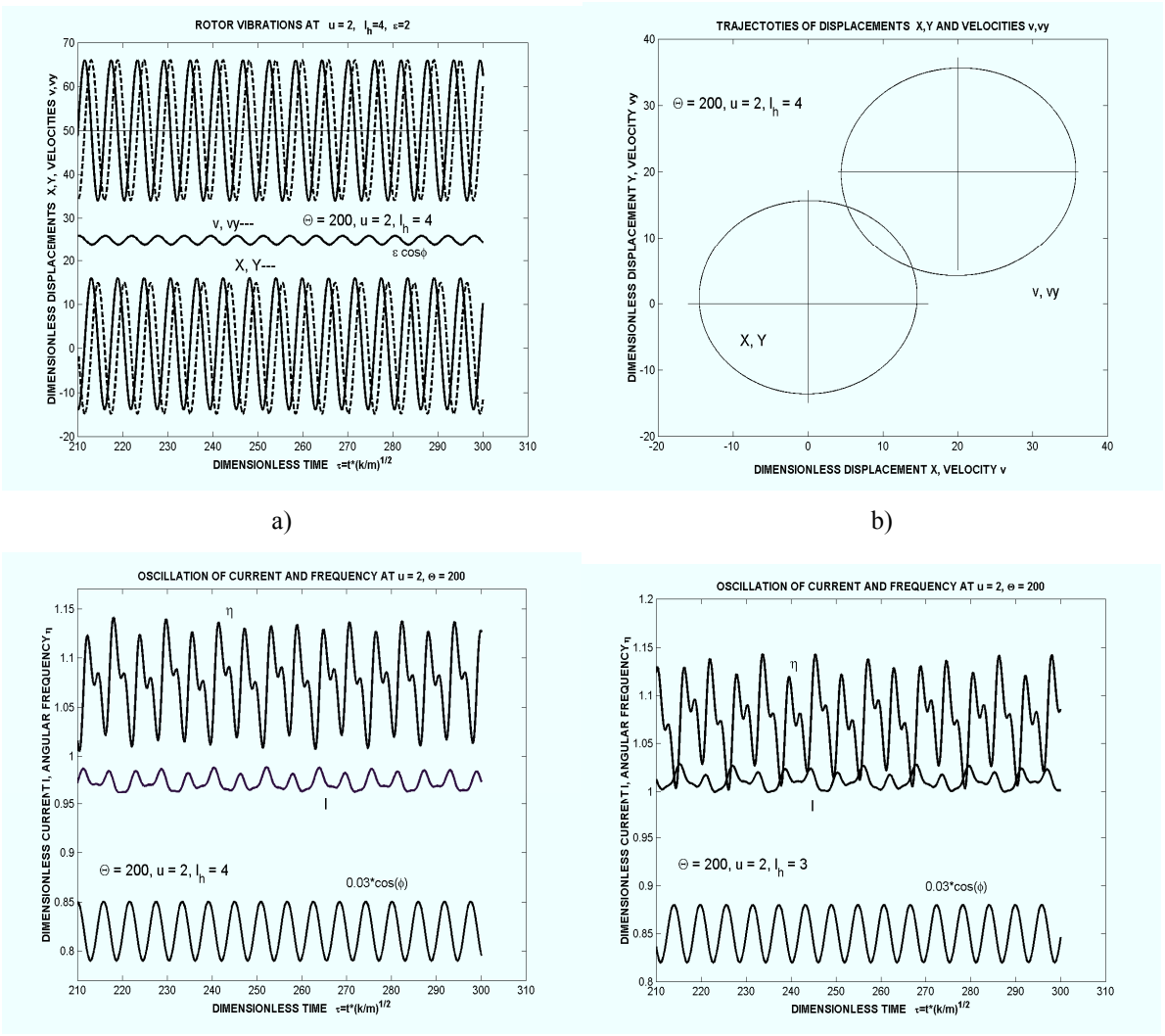

Fig. 3. Motion at high current parameters I_h, a) time history of rotor motion, b) disk centre trajectories,c) time history of current *I* and frequency η_j all at I_h=4, d) the same at I_h=3.

The adjacent figure 3d show the time histories of the same variables I, η, but for the lower current parameter $I_h = 3$. The increase of fluctuation of these variables is small, so that we can conclude that the influence of nonlinearity of the magnetic flux $\Phi(i)$ is negligible and the majority of distortion of mechanical and electrical variables are caused mainly by the limited power of driving motor. On the influence of nonlinear magnetic flux $\Phi(i)$ we can judge from the following diagrams calculated for lower values of current parameter I_h .

The influence of nonlinearity of magnetic flux $\Phi(i)$ reveals itself at current parameter $I_h = 2.7$ as seen from fig. 4 where in the part a) a small increase of current to the mean value $I \approx 1.05$ together with increase of its fluctuation occurs. Also the fluctuation of angular velocity η increases up to 50 % of its mean value. In comparison to the previous cases, the irregular oscillations of these both magnitudes is characterized by the increase of quasi-period from value 2 to approximately 15/6.5 = 2.3. This irregular fluctuation of frequency results however

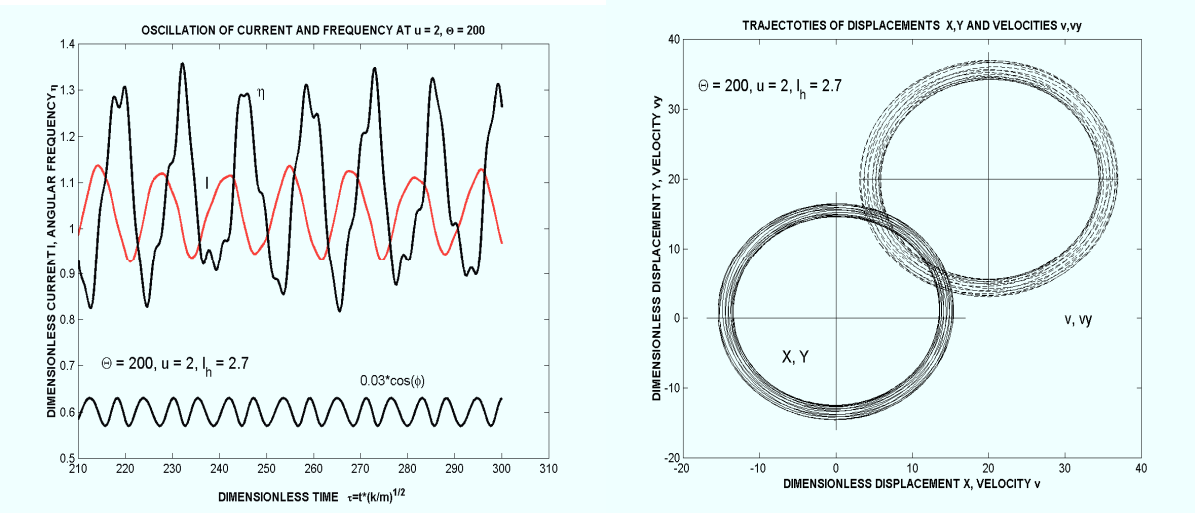

a) b)

Fig.4. Motion at I_h=2.7, a) current I and frequency η versus time τ, b) trajectories of rotor disk centre.

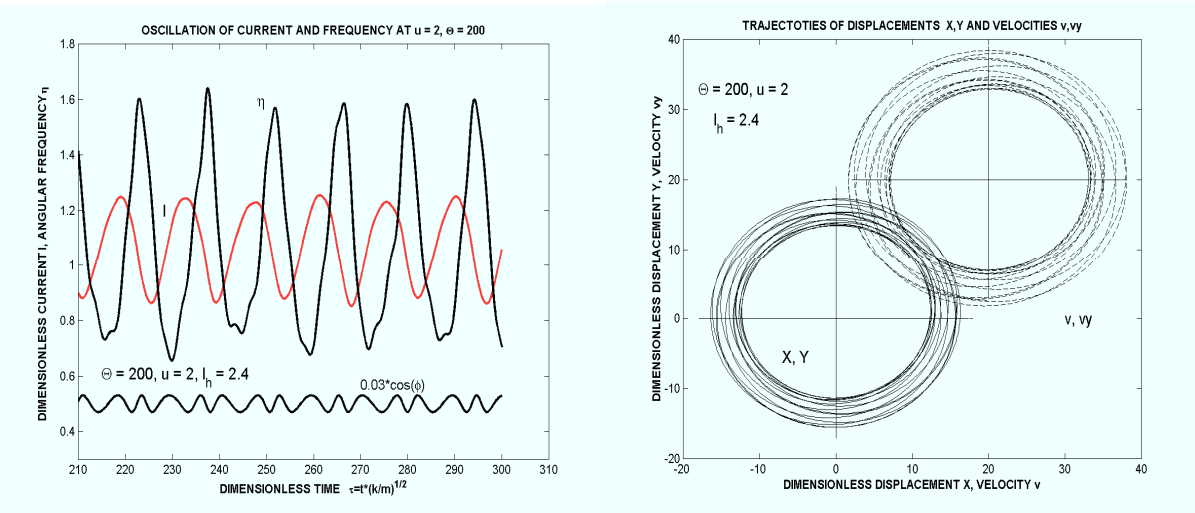

a) b)

Fig. 5. Motion at I_h=2.4, a) current I and frequency η versus time τ,. b) trajectories of rotor disk centre.

also in the small fluctuation of mechanical oscillations. It is small, but it is evident from the extended width of circular trajectories X, Y and v, vy in fig. 4b. The oscillations in coordinate X and Y are very near to harmonic, but they contain small quasi-periodic components.

The width of circular trajectories X,Y and v,vy increases to a well visible value (see fig. 5b) after decreasing the current parameter to I_h = 2.4. The quasi-periodic components which cause this distortion of harmonic oscillations of mechanical part – rotor – manifest themselves in large measure in the course of current $I(\tau)$ and of dimensionless frequency $\eta(\tau)$ as it is seen from fig. 5a. Irregular fluctuation of current $I(\tau)$ rises to 30 % of its mean value and also the fluctuation of frequency $\eta(\tau)$ increases to 75 %. The quasi-period T_{fluc} of these fluctuations increases very moderate to the ratio T_{fluc}/T_{rot} = 2.37, where T_{rot} is the mean period of rotor turning. Due to the large fluctuation of angular velocity η this period also strongly variable as it is seen from the lowest record in fig. 5a.

In the next fig. 6, there are presented results of calculations of system motion at current parameter I_h = 2.2. The large interval τ =0 – 300 of quasi-stationary course of current I and angular velocity η is shown in fig. 6a. Fluctuations of both variables again increase, as well as fluctuations of rotor vibrations shown in the next fig. 6b. These fluctuations increase to

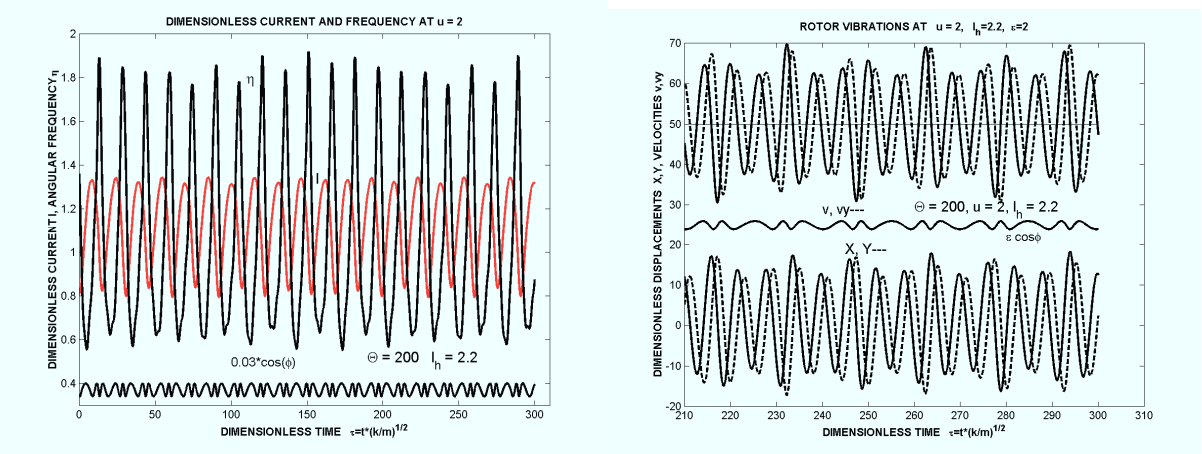

a) b)

c) d)

Fig. 6. Motion at I_h=2.2, a) long-time record of I and η, b) long-time record of rotor vibrations, c) plane trajectories of rotor centre, d) ZOOM record of I and η.

approximately 30% of the average amplitudes as shown from the trajectories in fig. 6c. The fluctuations of current I and angular velocity η in the last third of the time interval $0 - \tau_{max}$ is plotted in fig. 6d. These fluctuations are several times greater than those of mechanical rotor subsystem's vibrations. Current I fluctuates 50% and angular velocity η 120% of their mean values. Fluctuation of η is evident also from the bottom diagram of rotor revolutions.

Similar properties, but in a little increased measure, present the records shown in fig. 7 for the current saturation parameter $I_h = 2$. The main difference is the change from quasi-periodic to periodic motion with the three times higher period than is the average period of rotation. The period ratio is now integer: $T_{fluc} / T_{rot} = 3$. This periodicity is clearly seen from all sub-figures fig. 7a)b)c)d).

The large fluctuations of all physical magnitudes of investigated system were here realised for the demonstrative purposes by using a very low value of mechanical moment of inertia I_m [kg m^2] or in dimensionless value $\Theta = I_m / mx_{st}^2 = 200$. Sufficiently great moment of inertia

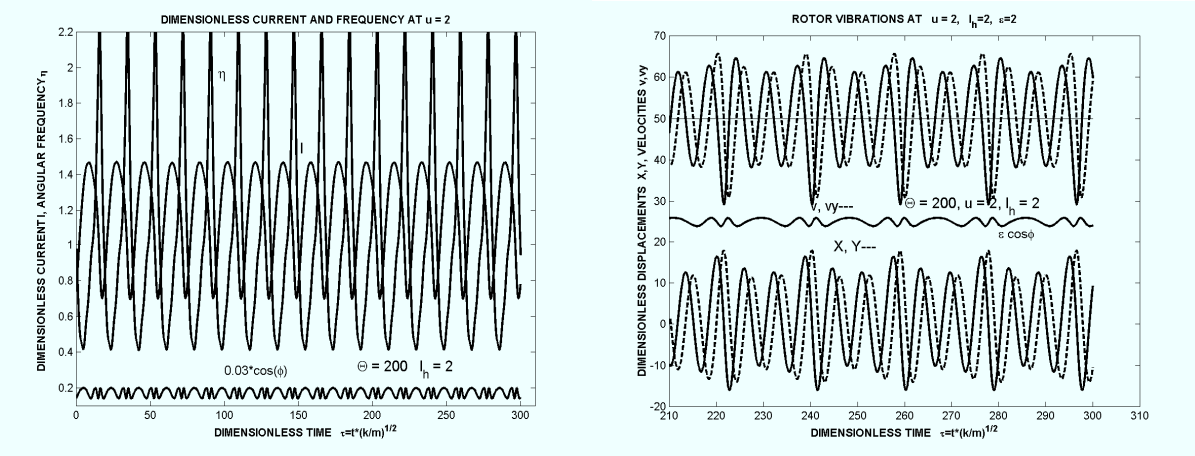

Fig. 7. Current parameter I_h=2, inertia moment Θ=200, a) I and η versus time τ, c) periodic plane trajectories of rotor, d) ZOOM record of I and η - continued.

reduces these fluctuations, as it is shown in the following figure, where responses on unbalance excitation at the same eccentricity $\varepsilon = e / x_{st} = 2$ and at the same current parameter $I_h = 2$ are shown. The fluctuation of angular velocity η decreases approximately 6 times, of current I 4 times. The amplitude fluctuation of rotor reduces to 18 % and the vibrations return to the quasi-periodic motion.

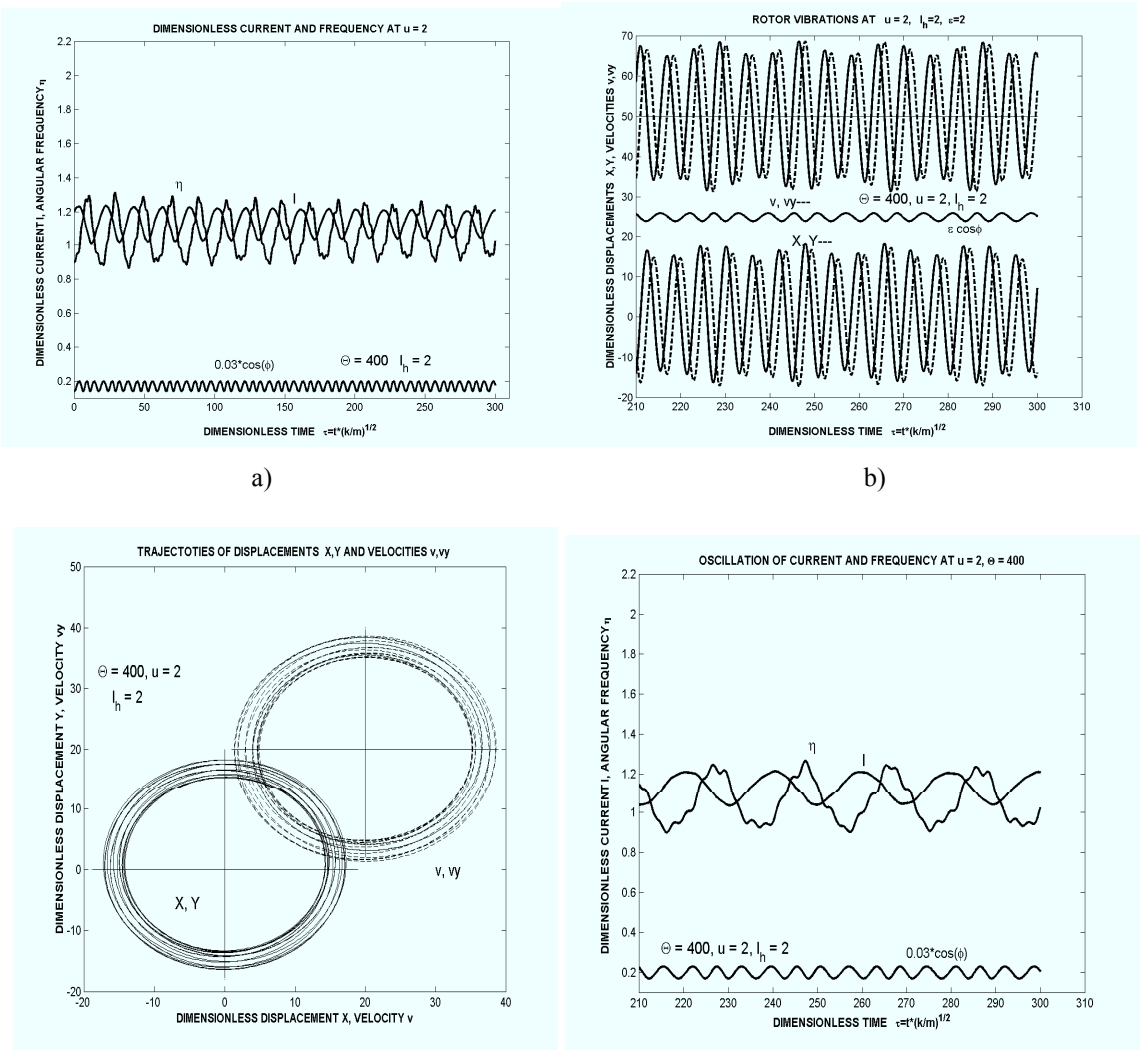

Fig. 8. Effect of increased moment of inertia Θ=400 at I_h=2, a) I and η versus τ, b) rotor vibration versus τ, c) rotor plane trajectories, d) ZOOM record of I and η – continued.

7. Conclusion

The discrete mathematical model of simple elastic rotor driven by an electric motor with limited power and limited moment of inertia was derived, transformed into dimensionless form and prepared for numerical solution. The investigation was focused on the effect of nonlinear magnetic flux on the mechanical vibration of rotor, on fluctuation of angular velocity and on variation of driving current at constant feeding voltage. As a model of nonlinearity describing the saturation of magnetic flux was applied the arc-tangent function with one control current parameter I_h.

Results are presented in the form of time histories of feeding current, angular velocity and in the form of plane trajectories of coordinates of rotor motion. Calculations of cases for different current parameters characterizing the nonlinearity of magnetic flux, show the great influence on the system motion.

The increasing nonlinearity causes the transfer of periodic to quasi-periodic motion with the ratio of fluctuation and rotation periods T_{fluc} /T_{rot} = 2–3. For the selected value of rotor moment of inertia, the fluctuations of electric current I in the motor and angular velocity η of rotor reach up ±50% of their mean values.

It is very important that the increase of moment of inertia of rotor strongly depresses the un-agreeable effect of saturation nonlinearity of magnetic flux.

Acknowledgements

This research was supported by the Grant Agency of CR, project No. 101/06/0063.

References

[1] J. M. Balthazar, et al., An Overview on Non-Ideal Vibrations, Meccanicca 38 (2003) 613 –621.
[2] V. O. Kononenko, Non-linear oscillations of mechanical systems, (in Russian), Naukova Dumka, Kiew, 1980.
[3] A. Muszynska, Ch. Hatch, D. Bently, Dynamics of Anisotropically Supported Rotors, International Journal of Rotating Machinery 3(2) (1997) 133 –142.
[4] L. Půst, Vibration of System Excited by a Motor with Limited Power, Proceedings of the 21st Conference Computational Mechanics 2005, Nečtiny, ZČU Plzeň, 2005, pp. 493 – 500.
[5] L. Půst, Influence of Electric Motors Characteristics on the Behaviour of Driven Systems, Proceedings of the Conference Engineering Mechanics 2005, Svratka, ČR, 12p. CD-ROM version, 2005.
[6] L. Půst, Weak excitation of non-linear rotor system with closely spaced resonances, Proceedings of the 12th IFToMM World Congress, Besancon (France), June, 2007, CD-ROM edition, pp. 504/1 – 504/6.